

Study of high pressure structural stability of CeO₂ nanoparticles^{*}

LIU Bo(刘波)¹ LIU Ran(刘然)¹ LI Quan-Jun(李全军)¹ YAO Ming-Guang(姚明光)¹
 ZOU Bo(邹勃)¹ CUI Tian(崔田)¹ LIU Bing-Bing(刘冰冰)^{1;1)} LIU Jing(刘景)²

¹ State Key Laboratory of Superhard Materials, Jilin University, Changchun 130012, China

² Institute of High Energy Physics, Chinese Academy of Sciences, Beijing 100049, China

Abstract: In situ high pressure XRD diffraction and Raman spectroscopy have been performed on 12 nm CeO₂ nanoparticles. Surprisingly, under quasihydrostatic conditions, 12 nm CeO₂ nanoparticles maintain the fluorite-type structure in the whole pressure range (0–51 GPa) during the experiments, much more stable than the bulk counterpart ($P_T \sim 31$ GPa). In contrast, they experienced phase transition at pressure as low as 26 GPa under non-hydrostatic conditions (adopting CsCl as pressure medium). Additionally, 32–36 nm CeO₂ nanoparticles exhibit an onset pressure of phase transition at 35 GPa under quasihydrostatic conditions, and this onset pressure is much lower than our result. Further analysis shows both the experimental condition (i.e., quasihydrostatic or non-hydrostatic) and grain size effect have a significant impact on the high pressure behaviors of CeO₂ nanomaterials.

Key words: CeO₂ nanomaterials, high pressure, experimental conditions, grain size effect, structural stability

PACS: 61.05.cf **DOI:** 10.1088/1674-1137/37/9/098003

1 Introduction

In recent decades, there has been a lot of interest in the high-pressure studies of nanostructured materials and their novel behaviors [1–3]. Previous studies indicate that phase transition pressures and processing of nanomaterials depend strongly on their grain size, shape, and structure [4–6]. They have been shown to have strong influence on critical pressures for phase transitions, phase transition routines, and even the amorphization processes [7, 8]. Recently, Gatta and his co-workers studied the elastic behavior of magnetite under high pressure using a mixture of methanol:ethanol:water=16:3:1 as pressure-transmitting medium. They found that elastic behaviors of Fe₃O₄ were strongly affected by the experimental conditions. At about 9 GPa, the bulk modulus of Fe₃O₄ exhibited a significant increase, and the pressure medium was largely solidified. Further study shows that the anomalous behavior of Fe₃O₄ is due to the non-hydrostatic condition caused by the solidification of the pressure medium [9]. Quirke et al. studied the pressure dependence of the radial breathing mode (RBM) of carbon nanotubes. They found that the pressure dependence of the shift in vibrational modes of individual carbon nanotubes is strongly affected by the nature of the pressure medium as a result of adsorption at the nanotube surface. The adsorbate is treated as an

elastic shell which couples with RBM of the nanotube via van der Waal interactions [10]. Hence, the hydrostatic or non-hydrostatic condition in high pressure studies plays a very important role in the behaviors of nanomaterials. Performing high pressure studies to explore how these conditions affect the nanomaterial behaviors is thus very important.

CeO₂ is an important material for numerous technological applications including catalyst, electrolyte, and solar cells due to its chemical stability, high oxygen storage capacity, etc [11]. Under ambient conditions, bulk CeO₂ crystallizes in cubic fluorite structure with (Fm3m) space group. It transforms into an orthorhombic α -PbCl₂ structure at a pressure of 31 GPa [12]. When the crystal size is decreased to nanometer scale, CeO₂ shows different behaviors in phase transition pressures and routines. Rekihi and co-workers performed high pressure studies on 12 nm CeO₂ nanoparticles up to 36 GPa using in-situ high pressure Raman technique. They found that the transition from cubic to orthorhombic phase occurred at 26 GPa, significantly lower than that for the bulk materials [13]. However, in their study, CsCl was adopted as pressure medium, and thus apparent non-hydrostatic conditions existed in the whole process of their high pressure experiments [13]. According to recent research, this non-hydrostatic condition was very likely to influence high pressure behaviors of CeO₂

Received 26 October 2012, Revised 18 December 2012

^{*} Supported by National Basic Research Program of China (2011CB808200), NSFC (10979001, 51025206, 51032001, 21073071, 11004075, 11004072, 11104105, 11079040), and Cheung Kong Scholars Programme of China

1) E-mail: liubb@jlu.edu.cn

©2013 Chinese Physical Society and the Institute of High Energy Physics of the Chinese Academy of Sciences and the Institute of Modern Physics of the Chinese Academy of Sciences and IOP Publishing Ltd

nanomaterials. So far, to our knowledge, there has been no report on the study of the effect of hydrostatic or non-hydrostatic conditions in the nano-CeO₂ system.

We have carried out high-pressure studies on 12 nm CeO₂ nanoparticles using in situ high-pressure X-ray diffraction under quasihydrostatic conditions. We found that under quasihydrostatic conditions (using a mixture of methanol:ethanol = 4:1 as the pressure medium), 12 nm CeO₂ nanoparticles maintain the fluorite-type structure up to 51 GPa, much more stable than that of bulk CeO₂ ($P_T \sim 31$ GPa) [12]. This finding is very different from previous studies [13–15]. Further analysis shows both the experimental conditions (i.e., quasihydrostatic or non-hydrostatic) and the grain size effect have significant impact on the high pressure behaviors of CeO₂ nanomaterials.

2 Experimental details

12 nm CeO₂ nanoparticles were prepared by a simple solvothermal method using n-butanol as solvent. All reactants used were analytical grade without any further purification. 1 mmol of Ce(NO₃)₃·6H₂O and 1 mL of NH₃·H₂O were loaded into a 50 mL Teflon-lined chamber which was filled with 40 mL of n-butanol. After being fully stirred to obtain a light brown solution, the autoclave was sealed and put inside an oven, which was maintained at 180 °C for 15 h and then cooled to room temperature naturally. The resulting yellow brown precipitates were separated by centrifuging and washed with distilled water and ethanol several times, respectively. The final product was dried in air at 60 °C for 24 h and collected for further characterization. A (HITACHI H-8100) transmission electron microscope (TEM) with accelerating voltage of 200 kV was employed to observe the morphology of the sample. X-ray powder diffraction (XRD) was used to characterize the product with Cu K α radiation ($\lambda=0.15418$ nm). When characterized by XRD, a scanning rate of 0.02° s⁻¹ was applied and the scanning range was 20°–90°. The Raman spectrum was recorded on a Renishaw inVia Raman Microscope in the backscattering geometry using the 514.5 nm line of an argon ion laser, provided with a CCD detector system. Raman bands were analyzed by fitting the spectra to Lorentzian functions to determine the line shape parameters.

In situ high-pressure X-ray diffraction experiments were carried out up to 51 GPa using a synchrotron X-ray source ($\lambda=0.6199$ Å) of the 4W2 High Pressure Station of Beijing Synchrotron Radiation Facility (BSRF). The diffraction data were collected using a MAR345 image plate. The two-dimensional XRD images were analyzed using the FIT2D software, yielding one-dimensional scattered intensity versus diffraction angle 2θ patterns, which were then analyzed by GSAS+EXPGUI Rietveld pack-

age to obtain unit cell parameters. The average acquisition time was 150 s. High pressure Raman spectra were measured using a Raman microscope (Renishaw inVia) with 514.5 nm laser excitation up to 50 GPa. All high-pressure measurements were performed at room temperature. Pressures were generated in a diamond anvil cell with a culet size of 300 μ m. The T301 stainless steel gasket was pre-indented by the anvils to an initial thickness of about 40 μ m, and a center hole of 100 μ m diameter was drilled as the sample chamber. A typical sample with a mixture of methanol and ethanol (4:1) as the pressure medium was loaded into the chamber, which provided a quasihydrostatic condition. Pressure was determined from the frequency shift of the ruby R1 fluorescence line.

3 Results and discussions

To characterize the morphology and structure of the CeO₂ nanoparticles, TEM and electron diffraction (ED) technique were carried out. Representative TEM micrographs of a typical product are shown in Fig. 1. These graphs reveal that all CeO₂ nanocrystals are monodisperse with an average size of 12 nm and a narrow diameter distribution. ED pattern (inset in Fig. 1) determines the polycrystalline nature of the product with a cubic fluorite structure.

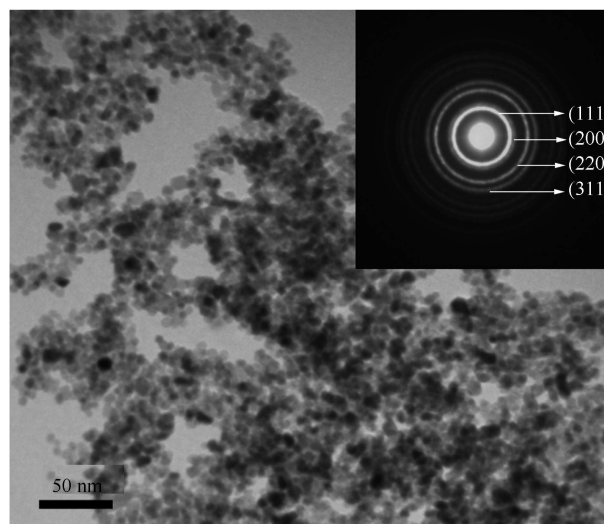


Fig. 1. The typical TEM and ED pattern of CeO₂ nanoparticles.

To determine the structure of the sample, XRD analysis was performed. Fig. 2 exhibits the XRD pattern of the CeO₂ nanoparticles. All detectable peaks in the pattern can be indexed to a pure cubic fluorite CeO₂ with a lattice constant $a=5.411$ (2) Å (JCPDS Card NO. 81-0792). According to the Debye-Scherrer formula, the strongest peak (111) at $2\theta = 28.575^\circ$, the peak (200) at

$2\theta=33.139^\circ$, the peak (220) at $2\theta=47.572^\circ$ and the peak (311) at $2\theta=56.402^\circ$ were used to calculate the average particle size of the CeO_2 nanoparticles, which was determined to be around 12 nm. These results are consistent with those obtained by TEM and ED analysis.

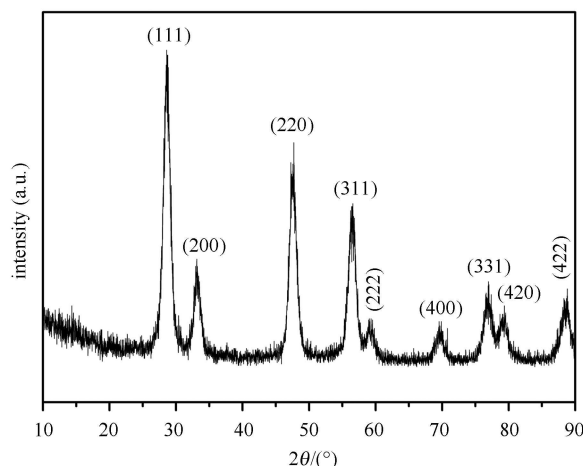


Fig. 2. The XRD pattern of CeO_2 nanoparticles.

Under ambient conditions, CeO_2 has a cubic fluorite type of structure and belongs to O_{5h} ($Fm\bar{3}m$) space group. There is only one triply degenerate Raman active optical phonon (F_{2g}), which gives only one first order Raman line at about 465 cm^{-1} . In the second order Raman spectrum, with nine phonon branches, there are 45 possible two phonon modes. The second order Raman peaks and their designations are 580 , 660 , 880 , 1030 and 1160 cm^{-1} for $\omega\text{TO}(X)+\text{LA}(X)$, $\omega\text{R}(X)+\text{LA}(X)$, $\omega\text{LO}+\omega\text{TO}$, $2\omega\text{R}(X)$ and $2\omega\text{LO}$, respectively [16].

Figure 3 shows the Raman spectrum of the CeO_2 nanoparticles with the fluorite phase within a range of $200\text{--}1200\text{ cm}^{-1}$ under ambient condition. A first order

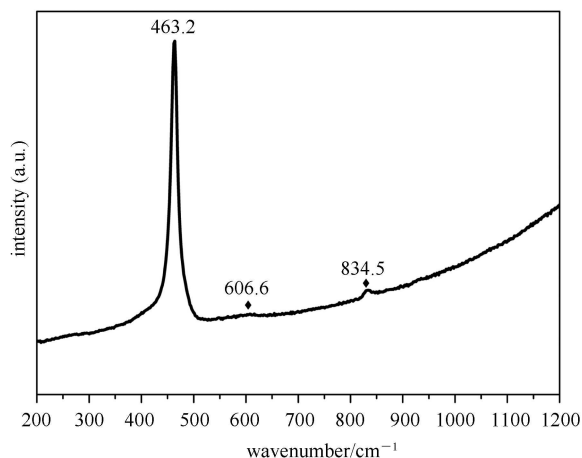


Fig. 3. The typical Raman spectrum of CeO_2 nanoparticles under quasihydrostatic condition using the mixture of methanol and ethanol (4:1) as pressure medium.

Raman peak (F_{2g}) at 463.2 cm^{-1} and a few second order Raman peaks at 606.6 and 834.5 cm^{-1} were observed. These results are consistent with the above studies.

Figure 4 shows in situ high-pressure X-ray diffraction patterns of the CeO_2 nanoparticles under quasihydrostatic conditions using the mixture of methanol and ethanol (4:1) as pressure medium. It clearly shows that the 12 nm CeO_2 nanoparticles maintain the fluorite-type structure in the whole pressure range (0–51 GPa), much more stable than the bulk counterpart ($P_T \sim 31\text{ GPa}$) [12]. In contrast, previous in situ high pressure Raman and XRD studies showed that 12 nm CeO_2 nanoparticles exhibited less stability than bulk CeO_2 , and had a phase transition pressure about 26 GPa [13, 14]. They used CsCl as the pressure medium and likely produced a non-hydrostatic condition. In order to illustrate our quasihydrostatic condition, we show the FWHM vs P in the whole pressure range. In Fig. 5, we can see that the XRD FWHMs almost remain constant in the whole pressure range, indicating the sample was under a quasihydrostatic condition. Thus, our comparative experiment shows that the quasihydrostatic or non-hydrostatic condition plays an important role in the high pressure behaviors of CeO_2 nanomaterials. Recently, S. Dogra et al. reported high pressure Raman study of CeO_2 nanoparticles using the mixture of methanol and ethanol (4:1) as pressure medium, and they found that 32–36 nm CeO_2 nanoparticles exhibited an onset pressure of phase transition at 35 GPa [15]. In contrast, our research shows that CeO_2 nanoparticles are more stable with smaller particle size ($\sim 12\text{ nm}$). The elevation of structural stability in the pressure-induced solid-solid phase transformation has been explained by the fact that smaller particle size leads to a higher surface energy between the phases involved in nanosized materials [17]. This result is in

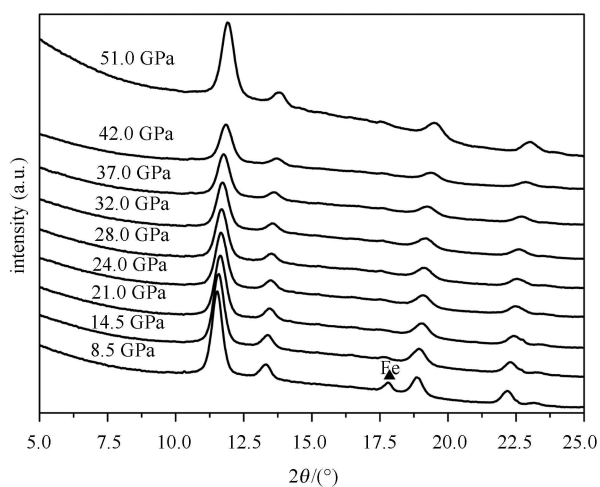


Fig. 4. In situ high-pressure X-ray diffraction patterns of 12 nm CeO_2 nanoparticles.

agreement with previous studies [18, 19]. Thus, our study shows that both the experimental conditions and the grain size effect have a strong impact on the high pressure stability of CeO₂ nanoparticles.

High pressure Raman spectra were collected for further studying the structural stability of 12 nm CeO₂ nanoparticles up to 50 GPa. Fig. 6 shows the in situ high-pressure Raman spectra of 12 nm CeO₂ nanoparticles. It is clearly observed in the whole pressure range, no other new peaks emerge, indicating that 12 nm CeO₂ nanoparticles maintain the cubic fluorite-type structure. The first-order fluorite peak (F_{2g}) shifts and slightly broadens with increasing pressure. It nevertheless still remains as the prominent peak up to 50 GPa. Fig. 7 exhibits the pressure dependence of Raman phonon frequency in the compression and decompression process from 0 to

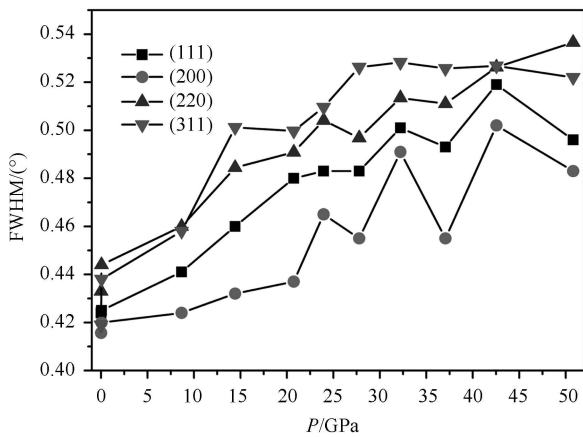


Fig. 5. The FWHM vs P of 12 nm CeO₂ nanoparticles.

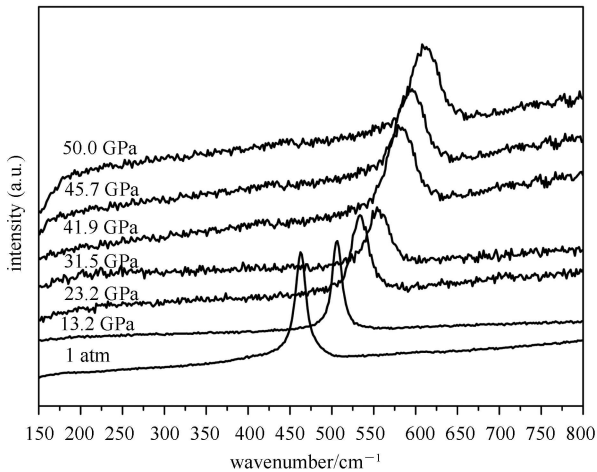


Fig. 6. In situ high-pressure Raman spectra of 12 nm CeO₂ nanoparticles.

50 GPa. During the compression to 50 GPa, we observed that the frequency of the first-order Raman peak increased with increasing pressure. Additionally, the change in this peak on decompression is similar to that in compression. This indicates there is no new phase in the decompression process. The high pressure Raman study is consistent with the high pressure XRD results.

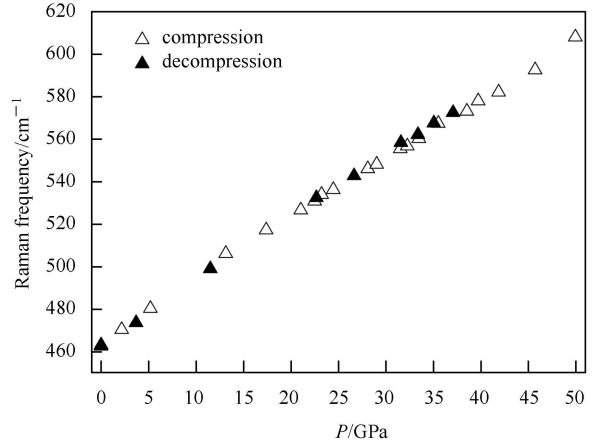


Fig. 7. The pressure dependence of the first-order Raman phonon frequency (F_{2g}) in the compression and decompression processes.

4 Conclusions

We studied the effect of experimental conditions (i.e., hydrostatic or non-hydrostatic) on the phase stability of CeO₂ nanoparticles through in situ high-pressure X-ray diffraction technology and high-pressure Raman spectra. Surprisingly, under quasihydrostatic conditions, 12 nm CeO₂ nanoparticles maintain the fluorite-type structure in the whole pressure domain (0–51 GPa), which is much more stable than the bulk counterpart ($P_T \sim 31$ GPa). In contrast, previous studies showed that 12 nm CeO₂ nanoparticles experienced phase transition at pressure as low as 26 GPa under non-hydrostatic conditions (adopting CsCl as pressure medium), and 32–36 nm CeO₂ nanoparticles elevated the onset pressure up to 35 GPa while under quasihydrostatic conditions. Further analysis shows the experimental conditions (i.e., hydrostatic or non-hydrostatic) as well as the grain size effect have a significant impact on the high pressure behaviors of CeO₂ nanomaterials.

We wish to thank Professor Keh-Jim Dunn for fruitful discussions and grammar revisions.

References

- 1 Grünwald M, Rabani E, Dellago C. *Phys. Rev. Lett.*, 2006, **96**: 255701
- 2 WANG, Zhen-Ling, QUAN, Ze-Wei, JIA Pei-Yun et al. *Chem. Mater.*, 2006, **18**: 2030
- 3 Hearne G R, ZHAO Jie, Dawe A M et al. *Phys. Rev. B*, 2004, **70**: 134102
- 4 San-Miguel A. *Chem. Soc. Rev.*, 2006, **35**: 876–889
- 5 WANG Yue-Jian, ZHANG Jian-Zhong, WU Ji et al. *Nano Lett.*, 2008, **8**: 2891
- 6 Wickham J N, Herhold A B, Alivisatos A P. *Phys. Rev. Lett.*, 2000, **84**: 923
- 7 WANG Lin, YANG Wen-Ge, DING Yang et al. *Phys. Rev. Lett.*, 2010, **105**: 095701
- 8 Wamy V, Kuznetsov A Y, Dubrovinsky L S et al. *Phys. Rev. Lett.*, 2009, **103**: 075505
- 9 Gatta G D, Kantor I, Ballaran T B et al. *Phys. Chem. Minerals*, 2007, **34**: 627
- 10 Longhurst M J, Quirke N. *Phys. Rev. Lett.*, 2007, **98**: 145503
- 11 LI Zen-Xing, LI Le-Le, YUAN Quan et al. *J Phys. Chem. C*, 2008, **112**: 18405
- 12 Kourouklis G A, Jayaraman A, Espinosa G P. *Phys. Rev. B*, 1988, **37**: 4250
- 13 Rekhi S, Saxena S K, Lazor P. *J Appl. Phys.*, 2001, **89**: 2968
- 14 WANG Zhong-Wu, Saxena S K, Pischedda V et al. *Phys. Rev. B*, 2001, **64**: 012102
- 15 Dogra S, Sharma N D, Singh J et al. *High Pressure Res.*, 2011, **31**: 292
- 16 Weber W H, Hass K C, McBride J R. *Phys. Rev. B*, 1993, **48**: 178
- 17 JIANG Jian-Zhong, Gerward L, Frost D et al. *J Appl. Phys.*, 1999, **86**: 6608
- 18 Qadri S B, YANG Jie, Ratna B R et al. *Appl. Phys. Lett.*, 1996, **69**: 2205
- 19 ZHANG Heng-Zhong, HUANG Feng, Gilbert B et al. *J. Phys. Chem. B*, 2003: **107**: 13051